Interferometric Three-Dimensional Imaging for Spinning Targets Based on Narrow-Band Radar

Chao Sun
School of Electronics and Information
Northwestern Polytechnical University
Xi'an, China
E-mail: sunchao13@126.com

Baoping Wang
Science and Technology on UAV Laboratory
Northwestern Polytechnical University
Xi'an, China
E-mail: wbpluo@sina.com

Yang Fang
School of Electronics and Information
Northwestern Polytechnical University
Xi'an, China
E-mail: fang_yang122@sina.cn

***Abstract*—In this paper, a novel interferometric 3-D imaging algorithm for spinning targets is proposed based on narrow-band radar. The height information of the scatterer is estimated by the phase difference between the same scatterer in two 2-D images generated by two antennas at closely-separated elevation angles via narrow-band radar imaging algorithms. For imaging of rapidly spinning targets, however, spurious peaks appear due to azimuth sample deficiency. Furthermore, the compressed sensing theory is applied into interferometric 3-D imaging based on joint sparsity of two images. The simulation results have proved the validity of the proposed algorithm.**

Keywords—Narrow-band radar; spinning targets; three-dimensional (3-D) imaging; compressed sensing

I. INTRODUCTION

For radar imaging of spinning targets, such as space debris, flying missiles, airscrews of airplane, conventional imaging approaches are invalid due to the violation of the rigid body assumption. However, spinning targets detection and imaging are essential to some special applications, such as missile defense, spacecraft safety, targets classification and recognition, etc. Recently, many investigators have devoted their work to high-resolution radar imaging of spinning targets. In [1]-[3], SRDI, SRMF-CLEAN, and SRIF imaging algorithms are proposed for 2-D imaging of spinning targets via narrow-band radar. Sample deficiency is usually inevitable in practice due to low pulse repetition frequency (PRF) radar and the existence of the shadowing effect, which will lead to generate aliased images. Thus, the newly compressed sensing (CS) theory [4]-[5] is applied into narrow-band radar imaging, improving the imaging performance greatly [6]-[7].

3-D images are capable of providing a more reliable description of target features and the identification of any given specific scatterers on the targets. Therefore, in [8]-[10], 3-D imaging algorithms are proposed for wide-band radars. In [8], the GRT-CLEAN algorithm makes use of the sinusoidal envelopes of the spinning scatterers in the range-slow time domain and obtains an image via noncoherent accumlation. Furthermore, the CLEAN technique is adopted in this algorithm for sidelobe reduction. A matched-filter-bank-based 3-D imaging algorithm is proposed in [9], based on target motion features. For a given matching parameter, a 2-D image slice is generated. Then, a series of 2-D image slices are obtained by changing the matching parameters of the matched filter bank, and finally, the 3-D target image is obtained. At the same time, a high-resolution 3-D imaging algorithm via the back-projection transform is proposed in [10], which makes use of both the sinusoidal envelope and phase information in the range-slow-time domain. Since the image is obtained via coherent accumulation, this algorithm is high in resolution and robust to additive noise. Although these algorithms are capable of providing high-resolution 3-D images and a more reliable description of target features, these algorithms based on wide-band radar are of high complexity and are difficult for real implementation of 3-D imaging. Besides, sample deficiency will lead to generate aliased images, influencing the target identification.

In this paper, a novel interferometric 3-D imaging algorithm for spinning targets is proposed based on narrow-band radar. This algorithm requires a radar system equipped with two receiving antennas. The echoes from the target are simultaneously received by the two receivers and are processed to obtain a pair of 2-D images, respectively, via narrow-band radar imaging algorithms. The height information of the scatterer is estimated by the phase difference between the same scatterer in two 2-D images. Furthermore, by defining a joint sparsity of image pairs, a CS algorithm is proposed to jointly form CS images, which can generate 3-D imaging result using limited measurements. At last, simulation results verify the effectiveness of the proposed algorithm.

II. INTERFERMETRIC 3-D IMAGING FOR SPINNING TARGETS BASED ON NARROW-BAND RADAR

A. Signal model

The discussion in this paper are based on the following assumptions. First, the translational motion of the spinning target is compensated completely. Second, the spinning speed is constant in the imaging interval. The geometry for interferometric 3-D imaging system is shown in Fig. 1. The two antennas O and A are located separately along the elevation direction, and the radar line of sight (LOS) is along the Y/Y' axis. The target angular velocity is Ω, with R as its spinning axis. α denotes the angle between R and the Y/Y' axis. 2-D image is a projection of a 3-D target onto 2-D imaging plane $X'O'Y'$. The angular velocity Ω is supposed to

This work was sponsored by the National Nature Science Foundation of China (NSFC) under Grants 61472324 and 61073106.

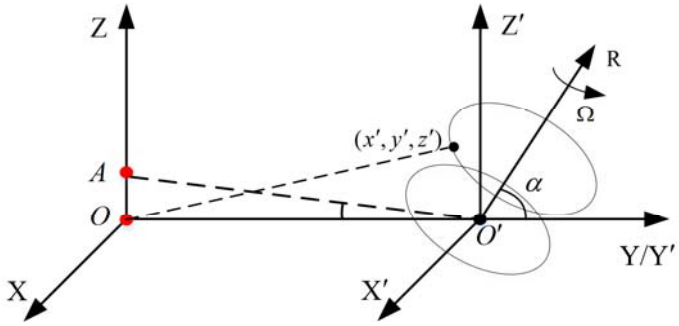

Fig. 1. The geometry of interferometric 3-D imaging system.

be estimated by autocorrelation method introduced in [1].

For narrow-band radar, the base-band signal at antenna $i(i \in \{O, A\})$ from a scatterer in the slow-time domain satisfies

$$s_i(\theta_n) = \sigma_i \exp\left(-j4\pi R_i(\theta_n)/\lambda\right) \tag{1}$$

where $\theta_n, n = 1,2,\cdots,N$ is the rotation angle in the imaging plane, σ_i is the reflectivity of the scatterer at the antenna i, λ is the wavelength, $R_i(\theta_n)$ is the instantaneous distance between the scatterer and the radar. Let the initial coordinates of the scatterer be (x', y', z'), according to Fig. 1, $R_i(\theta_n)$ satisfies

$$\begin{aligned} R_i(\theta_n) &= x'\sin\alpha\cos(\varphi_i)\sin(\theta_n) + y'\sin\alpha\cos(\varphi_i)\cos(\theta_n) \\ &\quad + z'\cos\alpha\sin(\varphi_i) \\ &= x\cos(\varphi_i)\sin(\theta_n) + y\cos(\varphi_i)\cos(\theta_n) + z\sin(\varphi_i) \end{aligned} \tag{2}$$

where α is constant in the imaging interval, the initial coordinates (x, y, z) of the scatterer remain unchanged in the 3-D imaging space. The imaging plane can be digitized by $x\cos(\varphi_i) = p\Delta x$, $y\cos(\varphi_i) = q\Delta y$, $p = 1,\cdots,P$, $q = 1,\cdots,Q$, where Δx and Δy are the pre-discretized grid space. Supposing Δx and Δy is sufficiently small with respect to the wavelength, all scatterers are located exactly on the pre-discretized grid. Then, (1) can be expressed as

$$\begin{aligned} S_i(\theta_n) &= \sum_{p=1}^{P}\sum_{q=1}^{Q}\sigma_i(p,q)\exp\left(-j\frac{4\pi}{\lambda}z\sin\varphi_i\right) \\ &\quad \exp\left\{-j\frac{4\pi}{\lambda}(p\Delta x\sin\theta_n + q\Delta y\cos\theta_n)\right\} \end{aligned} \tag{3}$$

B. Narrow-band radar 3-D imaging algorithm

The 2-D image can be obtained by applying complex-valued back-projection algorithm, which can be expressed as

$$\begin{aligned} \hat{I}_i(p,q) &= \sum_n\sum_i \sigma_i \exp\left(-j\frac{4\pi}{\lambda}z\sin\varphi_i\right) \\ &\quad \exp\left\{j\frac{4\pi}{\lambda}[(p_i'-p)\Delta x\sin\theta_n + (q_i'-q)\Delta y\cos\theta_n]\right\} \end{aligned} \tag{4}$$

where $\exp\left[j4\pi(p'\Delta x\sin\theta_n + q'\Delta y\cos\theta_n)/\lambda\right]$ is the phase-searching term, a peak value appears in the reconstructed image $\hat{I}_i$ when $p' = p$ and $q' = q$. On the other hand, no peak appears if $p' \neq p$ and $q' \neq q$ since the summation cannot be accumulated effectively.

Furthermore, after interferometric processing, the phase difference of the scatterer between two received signals can be expressed as follows

$$\Delta\phi = \frac{4\pi}{\lambda}z(\sin\varphi_O - \sin\varphi_A) \tag{5}$$

Since the baseline length is much shorter than the distance between the radar and the target, the elevation angle difference of the two antennas is quite small. Without loss of generality, $\varphi_A = \varphi_O + \Delta\varphi$, and $\Delta\varphi \ll 1$. Therefore, (5) is written as

$$\begin{aligned} \Delta\phi &= \frac{4\pi}{\lambda}z[\sin(\varphi_O + \Delta\varphi) - \sin\varphi_O] \\ &= \frac{4\pi}{\lambda}z[\sin\varphi_O\cos\Delta\varphi + \cos\varphi_O\sin\Delta\varphi - \sin\varphi_O] \\ &\approx \frac{4\pi}{\lambda}z\cos\varphi_O\Delta\varphi \end{aligned} \tag{6}$$

As a result, the height of the scatterer can be estimated by

$$z \approx \frac{\lambda}{4\pi\cos\varphi_O}\frac{\Delta\phi}{\Delta\varphi} \tag{7}$$

According to (7), the height information of each scatterer can be estimated by the phase difference between the corresponding pixels of two generated images from two closely separated antennas located along the elevation direction.

III. INTERFEROMETRIC 3-D IMAGING BASED ON CS

According to the Nyquist sampling theory, the radar PRF should be at least twice the Doppler bandwidth of the target returns in order to avoid Doppler spectrum aliasing. Thus the radar PRF should satisfy the following condition

$$PRF \geq 2f_{d\max} = 4R_{\max}\Omega/\lambda \tag{8}$$

where $f_{d\max}$ is the maximum of Doppler frequencies and $R_{\max}$ is the largest distance between some scatterer and the target center. For high speed spinning targets, the required radar PRF usually cannot be satisfied, and there usually exists the shadowing effect. In some sense, the insufficient PRF and shadowing effect will lead to azimuth under-sampling, which will lead to generate aliased images. Recently, the newly developed theory of compressed sensing (CS) raised by scholars presents a novel way to deal with this problem.

As the height estimation is estimated from a pair of 2-D images generated by two closely separate antennas, the first step of 3-D imaging is to generate 2-D images based on CS. Referring to (3), the received signal for each antenna can be rewritten as the following matrix form

$$S_i = \Phi I_i \tag{9}$$

where S_i is data matrix from ith antenna with the size of $N\times 1$, I_i with the size of $PQ\times 1$ denotes the image vector to be formed in the ith antenna, in which the corresponding scatterer's scattering characteristics of every element is as a

TABLE I. IMROVED OMP ALGORITHM

Improved orthogonal matching pursuit (OMP) algorithm
Input: S_O, S_A, Φ, the sparsity K or the residual energy $\|E\|_2$
Initialization: $I_O^0 = I_A^0 = 0$, $r_O^0 = S_O$, $r_A^0 = S_A$, $\Lambda = \varnothing$, $t = 1$
Iteration:
(1) $k_{\max} = \arg\max_k \left[\left\|\phi_k^* r_O^{t-1}\right\| + \left\|\phi_k^* r_A^{t-1}\right\|\right]$
(2) $\Lambda^t = \Lambda^{t-1} \cup \{k_{\max}\}$
(3) $I_O^t = \arg \min \|S_O - \Phi I_O\|_2$, $s.t.$ $\mathrm{supp}(I_O) \subseteq \Lambda^t$ $I_A^t = \arg \min \|S_A - \Phi I_A\|_2$, $s.t.$ $\mathrm{supp}(I_A) \subseteq \Lambda^t$
(4) $r_O^t = S_O - \Phi I_O^t$ $r_A^t = S_A - \Phi I_A^t$
(5) $t = t + 1$, stop if $k = K$ or $\min(\|r_O^k\|_2, \|r_A^k\|_2) \le \|E\|_2$
Output: $\hat{I}_O = I_O^t$, $\hat{I}_A = I_A^t$

vector of the dictionary Φ with the size of $N \times PQ$. The dictionary Φ can be defined as

$$\Phi_{N\times PQ} = \{\varphi_1, \varphi_2, \cdots, \varphi_{pq}, \cdots \varphi_{PQ}\},$$
$$\varphi_{pq} = \exp[-j\frac{4\pi}{\lambda}(p\Delta x \sin\theta_{N\times 1} + q\Delta y \cos\theta_{N\times 1})] \quad (10)$$

Each pixel of the reconstructed image can be denoted as $I_i(pq) = \sigma_i(pq)\exp(-j4\pi z_{pq}\sin\varphi_i / \lambda)$, and each non-zero pixel represents one scattering center located on the target. Generally, the whole non-zero pixels occupy only a small part of the image plane, which motivates the CS theory to reconstruct $\hat{I}_i$ from S_i. One way to reconstruct two radar images is to apply CS independently for each antenna. In fact, the relative phase information may not be preserved on account of the possibility of shifts between the two images. Therefore, we propose another way to solve this problem. By defining a global sparsity of image pairs and defining a CS method that jointly forms CS radar images, scattering centers are located in the same pixels in both images.

Since the two images share the same sparsity support, that is to say, the scattering centers are located on the same positions in both images, we define the following joint-sparsity constraint as

$$\|I\|_0 = \|\,|I_O| + |I_A|\,\|_0 \quad (11)$$

where $\|I\|_0$ represents the joint-sparsity. According to (11), we take the sum of the two images as the common sparsity support, and then we can reconstruct the two images constrained by (11), which can be formulated as

$$\min_{(I_O, I_A)} \|I\|_0 \quad s.t. \begin{cases} \|S_O - \Phi I_O\|_2 \le \varepsilon \\ \|S_A - \Phi I_A\|_2 \le \varepsilon \end{cases} \quad (12)$$

where ε is chosen according to the channel with lower noise level to make sure that good radar images can be obtained for each antenna. In the case of this paper, (12) can be solved by an improved orthogonal matching pursuit (OMP [11]) algorithm, and the detailed procedures are given in Table I.

IV. SIMULATION RESULTS

In this section, simulation experiments are carried out to test the proposed 3-D imaging algorithm. The radar carrier frequency is 10 GHz and the system bandwidth is 20MHz, giving a range resolution of 7.5m. A target composed of nine scattering centers with the same unit amplitude reflectivity function is simulated, as shown in Fig. 2(a). A pair of antennas with elevation angles 0° and 0.01° are used to simulate the interferometric system. The target rotates at a frequency of 15Hz and the maximum rotation radius is 0.2 m. According to (8), the required PRF for non-aliased imaging is 2513 Hz. The imaging interval is 0.5 s and the number of azimuth samples is 1256. Since a narrow-band waveform is transmitted, the range profile is still within a single range cell after range compression. Fig. 2(b) shows the 3-D reconstruction result by complex-valued back-projection (CBP) algorithm. As can be seen, the positions of the scattering centers in the X direction and Y direction can be estimated accurately, and the estimated height information only provide overall shape, which cannot provide correct values due to interaction between scattering centers. However, the CS-based algorithm can reconstruct the 3-D positions of scattering centers accurately, as shown in Fig. 2(c).

Besides, sample deficiency is usually inevitable in practice due to low PRF radar and the existence of the shadowing effect, which will lead to generate aliased images. We reduce the PRF to a quarter of the required value (628 Hz). The imaging interval is 0.25s and the number of target sample 157. For scatterers on each floor, the back-scattering coefficients are 0.4, 0.8 and 1 respectively according to their distances from the target center. 3-D images obtained via the CBP-based algorithm and the CS-based algorithm are shown in Fig. 3(a) and (b) respectively. A comparison shows that the CBP-based algorithm only can estimate the positions of strong scatterers, while the CS-based algorithm can estimate 3-D positions of all scatterers with small errors.

V. CONCLUSION

This paper derives a class of geometrical and signal models for narrow-band radar interferometric 3-D imaging for spinning targets, and proposes CBP-based and CS-based 3-D imaging algorithms. The CS-based algorithm can estimate the height information more accurately than the CBP-based algorithm. More importantly, when the required PRF cannot be satisfied, the CS-based algorithm can still estimate the 3-D positions of the scattering center. At last, numerical simulation are provided to validate the effectiveness of the proposed method. Further, the effectiveness of the proposed algorithm still needs to be tested with real measured radar data.

ACKNOWLEDGMENT

The authors would like to thank the handing editor and the anonymous reviewers for their valuable and helpful comments.

REFERENCES

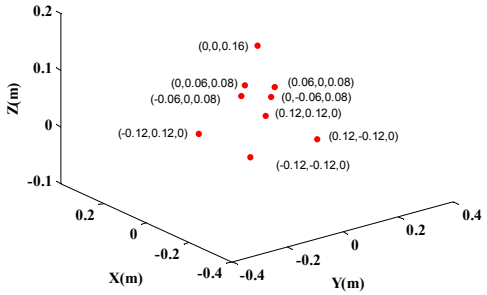

(a)

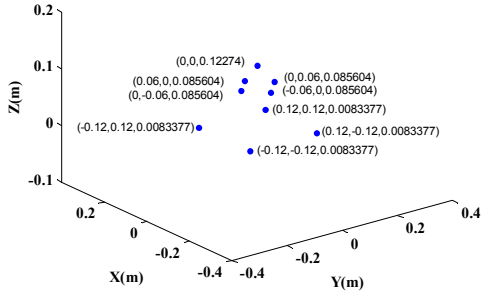

(b)

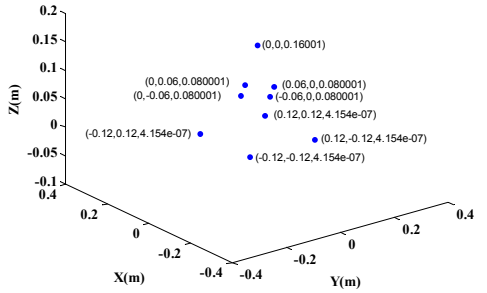

(c)

Fig. 2. Comparison of imaging results without sample deficiency. (a) Target distribution. (b) CBP-based algorithm. (c) CS-based algorithm.

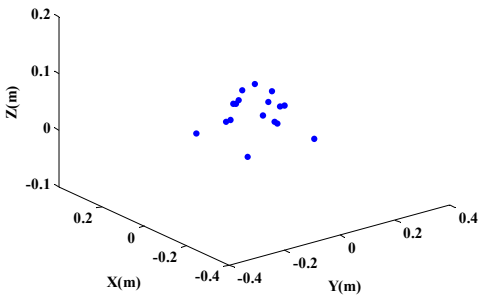

(a)

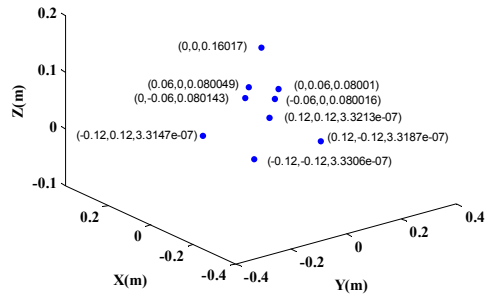

(b)

Fig. 3. Comparison of imaging results with sample deficiency. (a) CBP-based algorithm. (b) CS-based algorithm.

Letters., vol. 7, no.4, pp. 626-630, October 2010.

[4] D. Donoho, "Compressed Sensing," IEEE Trans. Inf. Theory, vol. 52, no.4, pp.1289-1306, April 2006.

[5] E. Candès, J. Romberg, and T. Tao, "Robust uncertainty principles: exact signal reconstruction from highly incomplete frequency information," IEEE Trans. Inf. Theory, vol. 52, no. 2, pp. 489-509, February 2006.

[6] X. Bai, G. Sun, Q. Wu, M. Xing, and Z. Bao, "Narrow-band radar imaging of spinning targets," Sci. China Inf. Sci., vol. 52, no. 4, pp. 873-883, April 2011.

[7] L. Hong, F. Dai, and H. Liu, "Sparse Doppler-only snapshot imaging for space debris," Signal Process., vol. 93, no. 4, pp. 731-741, April 2013.

[8] Q.Wang, M. Xing, G. Lu and Z. Bao, "High-Resolution Three-Dimensional Radar Imaging for Rapidly Spinning Targets," IEEE Trans. Geosci. Remote Sens., vol. 46, no.1, pp. 22-30, January 2008.

[9] M. Xing, Q. Wang, G. Wang and Z. Bao, "A Matched-Filter-Bank-Based 3-D Imaging Algorithm for Rapidly Spinning Targets," IEEE Trans. Geosci. Remote Sens., vol. 47, no.7, pp. 2106-2113, July 2009.

[10] X. Bai, M. Xing, F. Zhou and, G. Wang, and Z. Bao, "High-Resolution Three-Dimensional Imaging of Spinning Space Debris," IEEE Trans. Geosci. Remote Sens., vol. 47, no.7, pp. 2352-2362, July 2009.

[11] D. Needell, and R. Vershynin, "Uniform uncertainty principle and signal recovery via regularized orthogonal matching pursuit," Found. Comput. Math., vol. 9, no. 3, pp. 317-334, June 2009.